Available online at www.sciencedirect.com

ScienceDirect

Procedia CIRP 65 (2017) 13 – 18

www.elsevier.com/locate/procedia

3rd CIRP Conference on BioManufacturing

Multi-layered scaffolds production via Fused Deposition Modeling (FDM) using an open source 3D printer: process parameters optimization for dimensional accuracy and design reproducibility

E. Ceretti[a], P. Ginestra[a*], P.I. Neto[b], A. Fiorentino[a], JVL Da Silva[b]

[a]*Department of Mechanical and Industrial Engineering- University of Brescia – Via Branze 38, 25123 Brescia - Italy*

[b]*Centro de Tecnologia da Informação Renato Archer – CTI - Rodovia Dom Pedro I, Km 143,6 - Amarais, SP, 13069-901, Brasil*

* Corresponding author. Tel.: +390303715538; *E-mail address:* paolaserena.ginestra@gmail.com

Abstract

One of the most applied strategies in tissue engineering consists in the development of 3D porous scaffolds with similar composition to the specific tissue. In fact, the microstructure of the scaffolds influences the final structure of the in growing tissue. In this study, multi-layered PCL scaffolds were produced with modified Fab@home FDM printer in order to analyze the influence of the extrusion technology (filament or powder extrusion head) and of the process parameters on the deposited material. In particular, dimensions and uniformity of both deposited filament and grid of the scaffolds were analyzed to understand the influence of the process parameters so as to optimize the FDM production technology.

Peer-review under responsibility of the scientific committee of the 3rd CIRP Conference on BioManufacturing 2017

*Keywords:*3D printing, fused deposition modeling, scaffold, polymers, fibroblasts.

1. Introduction

Highly porous scaffolds are required to provide the three-dimensional growth of cells in an organized way. The morphology and microstructure of the scaffolds need to mimic the final shape and structure of the organs and tissues that need to be rebuilt, so they must satisfy specific mechanical and biological requirements in structure, surface morphology that promotes cell-cell and cell-matrix interactions, proper porosity, pore size, pore distribution and pore interconnectivity [1-2]. Additive layer biomanufacturing technologies are increasingly recognized as ideal techniques to produce 3D structures with controlled pore size, spatial distribution and interconnectivity, providing an adequate mechanical support for tissue regeneration while supporting in-growing tissues [3-7]. Construction of the scaffold is usually done using technologies like Fused Deposition Modeling (FDM) [8, 9]. The extrusion-based strategies to produce highly interconnected pore structures and the effect of such structures in promoting cells proliferation were explored by several researchers [10-13]. However, during the fabrication process, materials are subjected to phase changes under relatively high temperature. Moreover, the shear rates during the extrusion process are considered relatively high [14]. The processing conditions considered for each application may affect the required geometry as a result of the transformations in the material during the extrusion. This case study was focused on producing multi-layered scaffolds with the open source Fab@Home 3D printer [15, 16] that was customized and equipped with two exchangeable FDM extrusion heads. In particular, the two heads process grain and wire bulk material respectively and were used to fabricate poly-caprolactone (PCL) grids. The sizes of the grids pores were chosen on the basis of the typical final application of 3D scaffolds with structured porosity [17]. The influence of grid dimensions, FDM technology and process parameters on the scaffolds

Peer-review under responsibility of the scientific committee of the 3rd CIRP Conference on BioManufacturing 2017
doi:10.1016/j.procir.2017.04.042

precision and uniformity was analyzed, so to optimize FDM process and also to identify the influence of some of these parameters on grid formation and extrusion of the filament. The realized grids were observed under optical microscope and measured in terms of diameter of the deposited strand and dimension of the pores. The statistical analysis on the results was carried out to consider the effects of each factor and their interactions on the scaffold geometry to gain a better reproducibility and repeatability of the part. Moreover, the comparison between the two FDM processes (grain and wire) allowed identifying the most suitable production technology in terms of robustness. Finally, the authors propose the use of these statistical models to optimize the bio-manufacturing process used to produce multi-layered scaffolds that have been demonstrated to play an important role in promoting cells attachment, migration, and proliferation in a 3D culture formation.

2. Scaffold design and FDM process

2.1. Definition of the geometry

The geometry of the 3D printed structures is characterized by equidistant filaments in the X and Y directions forming a squared grid. In particular, the side of the grid pores (h_0) is equal to the distance between the filaments (namely air gap) and the height of the pores (Δz) is the displacement of the extrusion head in the Z axis between two layers (namely path height).

A total of three configurations was considered. In particular, the configurations are characterized by different distances between the filaments h_0 and path height Δz. The configurations A, B and C (Fig. 1) are characterized by squared pores having three different sides (h_0) equal to 0.6 mm, 0.8 mm and 1.0 mm respectively. Three path heights were chosen for each configuration equal to 0.3 mm, 0.4 mm and 0.5 mm. The whole grid of each configuration has a 10x10 mm^2 area.

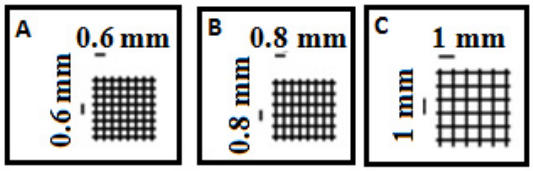

Figure 1 Imposed pattern configurations: A, B and C.

2.2. FDM tests

The grid samples were realized by the FDM printer Fab@home [18]. The printer is controlled by a software where it is possible to set the displacement of the extrusion head in the X,Y and Z axes. In particular, the displacement of the head in the X and Y-axes determines the distance between the filaments borders (h_0) while the displacement in the Z axis is defining the width of the deposited filament (Δz). Two extrusion heads were used in this work: a wire and a grain extrusion head (Fig. 2 and 3). Both the heads are designed and developed at CTI Lab and are characterized by a nozzle of 0.4 mm.

The printing parameters set to obtain the selected configurations are reported in Table 1 and Table 2.

Three repetitions were fabricated for each process parameters set.

Table 1 Designed printing configuration.

Side of the pores h_0 (mm)	Path height Δz (mm)
0.6	0.3
0.6	0.4
0.6	0.5
0.8	0.3
0.8	0.4
0.8	0.5
1	0.3
1	0.4
1	0.5

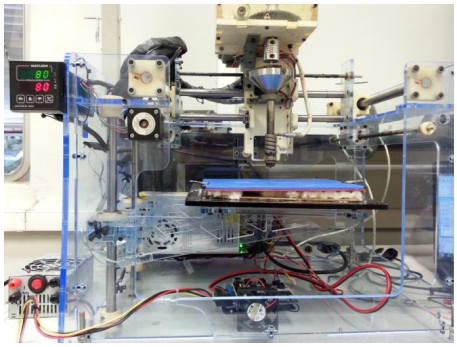

Figure 2 Fab@home printer with the grain extrusion head using a microscrew.

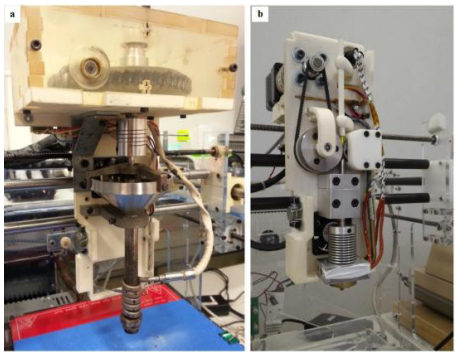

Figure 3 The used extrusion heads: a) grain and b) wire.

Table 2 Designed printing process.

Parameter	Description	Set value
DR	Deposition Rate	0.01
PS (mm/s)	Path Speed	5
# layers	Number of layers	4
T (° C)	Extrusion temperature	90 (wire) 80 (grain)

3. Scaffold characterization

3.1. Sample measuring

The FDM samples were observed using the Mitutoyo Quick Scope QS-200z optical microscope system.
The optical microscope was used to analyze the details of the structures. Fig. 4 and Fig. 5 show the samples obtained with the wire extrusion and the powder extrusion heads respectively. Then, the microscope images were processed with ImageJ software [19] to measure the grid dimensions. Approximately 60 measures were taken on the whole grid area in terms of filament diameters and pore dimensions. Then, their average values, d and h, and standard deviations, σ(d) and σ(h), within the sample were calculated.

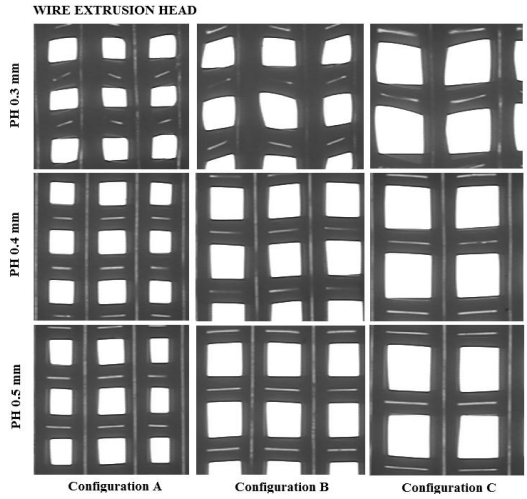

Figure 4 Optical microscope images 0.5x of the PCL grids produced with the wire extrusion head.

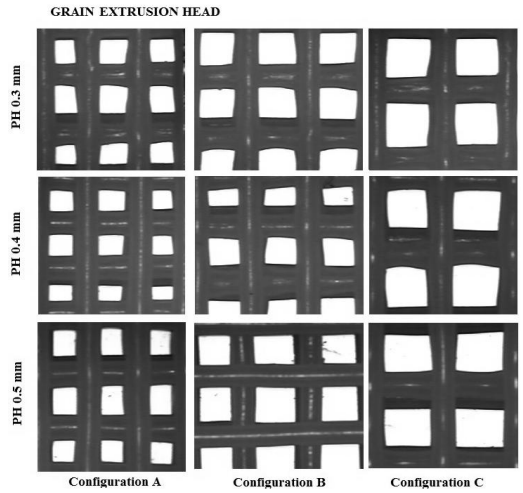

Figure 5 Optical microscope images 0.5x of the PCL grids produced with the grain extrusion head.

3.2. Statistical analysis

The measured data were statistically analyzed using ANOVA in order to identify the process parameters that significantly affect the dimensions and the precision of the FDM scaffolds (p-value $\leq$ 0.5). In particular, hierarchic general linear models were adopted for the analysis and, when the ANOVA hypotheses were not respected, Box-Cox transformations were used to analyze the responses. The analysis was based on three factors: the technology (corresponding to the type of the extrusion head that was used), the nominal displacement of the extrusion head in the Z axis (Δz) and the nominal side of the pores (h_0). Moreover, the influence of the machine axes (X and Y) on the pore dimension was considered.
Table 3 and Fig. 6 to Fig. 10 report the summary of the analysis. In particular, the main effects plot in Fig. 6 shows that the diameter (d) is strongly influenced by the nominal side of the pores (h_0) and in particular the diameter decreases as the distance between the filaments is increased. This effect is probably caused by the deposition of the filament in the gaps (pores) between two subsequent filaments where the diameter is stretched and becomes thinner. The interaction plot reported in Fig. 7 shows that the diameter d is more robust when the grain extrusion head is used, due to the low dependence of the diameter on the value of h_0. Moreover, the optimal process parameters set that leads to the closest results by using the two extrusion heads is set at intermediate values of h_0 (0.8 mm) and higher values of Δz (0.5 mm). The main effect plot on the standard deviation of the diameter σ(d) (Fig. 8) confirms the robustness of the grain extrusion head with respect to the deposited diameter.
Therefore, from the analysis of the dispersion of the data of the diameter it can be concluded that the process results more uniform for the grain extrusion head. These results confirm that the grain extrusion system is more stable for this type of application.

Table 3. Summary of the factors that affect the FDM process (+) and included in the model for hierarchy (°).

		Factors			
Outcome	**Box-Cox**	***Technology (A)***	***h_0 [mm] (B)***	***Δz [mm] (C)***	***Axis (D)***
d	d^{-1}	°	+	°	n.a.
σ(d)	$\sigma(d)^{0.5}$	+			n.a.
h	$h^{-0.5}$	+	+	+	°
σ(h)	$\sigma(h)^{-0.5}$	+	+		°

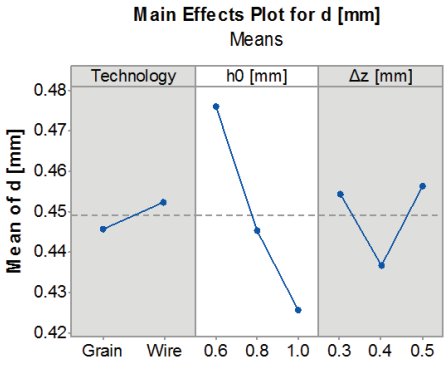

Figure 6 Main effects plot for the extruded diameter of the filament. White background refers to influencing factors.

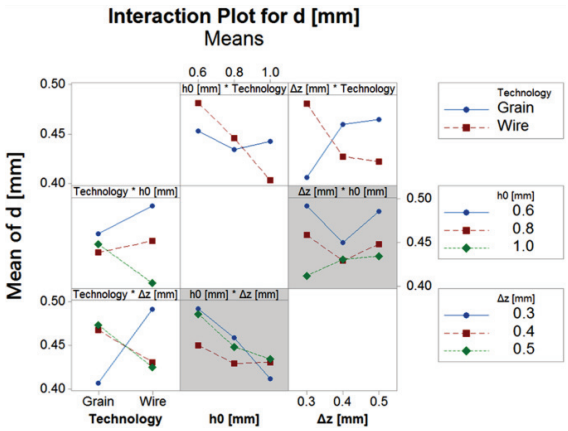

Figure 7 Interaction plot for the diameter of the filament extruded. White background refers to influencing factors.

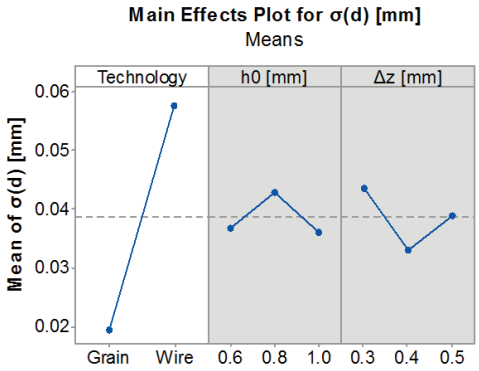

Figure 8 Main effects plot for the standard deviation of the diameter of the filament extruded. White background refers to influencing factors.

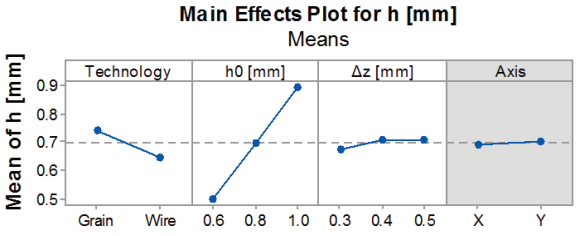

Figure 9 Main effects plot for the side of the pores (h). White background refers to influencing factors.

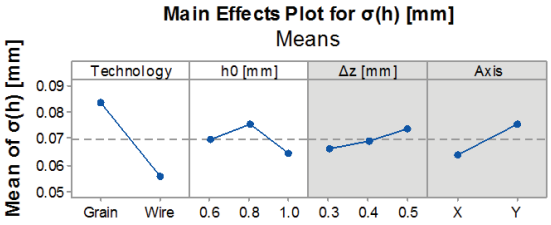

Figure 10 Main effects plot for the standard deviation values of the side of the pores (h).

The results of the analysis on the side of the pores are shown in Fig. 9 and Fig. 10. In this case, the axis factor was considered to analyze the effect of the displacement of the extrusion head along X and Y-axes. As shown in Fig. 9, the side of the pores h is mainly influenced by its controlling factor (h_0), which indicates a good stability of the process. The interaction plot is not reported due to the absence of relevant technological interactions between the factors. The main effect plot on the standard deviation of the side of the pores σ(h) is reported in Fig. 10. In this case, the process results more uniform for the wire extrusion head.

In general, the statistical analysis shows that the extrusion head influences the uniformity of the deposited grid. In particular, the diameter is enhanced by the use of the grain extrusion head while the uniformity of the side of the pores is enhanced by the use of the wire extrusion head. Nevertheless, by analyzing the values of the standard deviations in both cases, it can be noticed that the imprecision of the printer is more evident on the obtained side of the pores than in the diameter of the extruded filament. Therefore, the grain extrusion head is preferable for this type of applications and assures the process stability during the extrusion of this polymer.

4. Cell culture preliminary tests

To verify the effectiveness of the produced scaffolds, Human Foreskin Fibroblasts (HFF) cells were seeded at a cellular density of 40,000 cells/cm^2. The concentrated cell suspension was deposited onto a scaffold of configuration A (grain head) and incubated for 45 min before filling the culture dish with the culture medium. The cells were cultured using Dulbecco's modified Eagle's medium supplemented with 15% fetal bovine serum, 100 IU/ml penicillin, 100 µg/ml streptomycin and 2 mM L-glutamine. All cell culture reagents were purchased from Thermo Fisher Scientific. Cells were maintained at 37 °C in a saturated humidity atmosphere containing 95% air and 5% CO2. Before cell seeding, all the scaffolds were sterilized under UV light. Cell adhesion was microscopically evaluated 24 hours after seeding. The samples were tested using optic microscope for cell static culture highlighting the full recognition of the PCL grid in terms of cellular spreading and the proliferation grade of the cells. Fig. 11 shows the HFF on the PCL filaments as a result of a complete adhesion of the cells on the structure. The

colonization of the structure is validated by the presence and the integrity of a complete monolayer of cells.

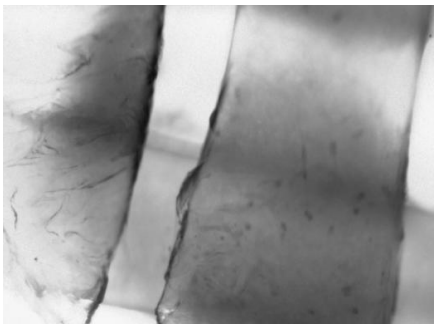

Figure 11 Optical microscope image 5X of the HFF cells seeded on the PCL filaments scaffolds of configuration A.

5. Discussion and conclusions

The paper analyzes the effects of the process and dimensional parameters on the production of PCL multilayer scaffolds via fused deposition modeling with an open source 3D printer. A wire and a grain extrusion heads were used making a comparison between the two extrusion processes. The analysis is focused on the dimensional differences between three imposed geometric configurations and the final product characteristics. In particular, optical microscope images were processed to measure the scaffolds dimensions and data were analyzed using ANOVA. In particular, the statistical analysis performed on the diameter of the extruded filament and the resulting side of the pores, highlighted that the process tends to be more stable by using the grain extrusion head. As a matter of fact, the diameter of the extrusion head is influenced by the nominal side of the pores and results more uniform and more robust with respect to other process parameters when the grains are extruded. On the other hand, the statistical analysis performed on the obtained side of the pores showed that the process is stable and more uniform when the wire extrusion head is used. Nevertheless, the imprecision of the printer is more evident on the obtained side of the pores than in the diameter of the extruded filament. From the results of the ANOVA analysis it can be concluded that the technology, in terms of the used extrusion head, is not strongly affecting the resulting geometry of the samples. Therefore, different extrusion processes can be used for various type of materials according to production and application necessities. However, the grain extrusion head is preferable for the investigated application and assures the process stability during the extrusion of the poly-caprolactone. The biological characterization of these structures shows that, despite the hydrophobicity of the polymer, human fibroblasts seeded on the grids are able to complete colonize the scaffolds. The promising results lay the foundations for the production of hybrid 3D scaffolds by the integration of the FDM and the electrospinning techniques. The future work will be focused on the thermally controlled adhesion of PCL FDM layers and PCL electrospun layers. The resulting hybrid structures will be subjected to dynamic cell co-culture tests in a bioreactor chamber to evaluate the effects of the different scaffolds configurations in terms of cell colonization during osteo-chondral tissue engineering applications.

Acknowledgements

The authors would like to acknowledge the support and the assistance of Prof. Patrizia Dell'Era of University of Brescia.

References

[1] Ginestra P, Ceretti E, Fiorentino A. Electrospinning of poly-caprolactone for scaffold manufacturing: experimental investigation on the process parameters influence. Proc. CIRP 2016; 49: 8-13.
[2] Ginestra PS, Ghazinejad M, Madou M, Ceretti E. Fabrication and characterization of polycaprolactone-graphene powder electrospun nanofibers. Proc. SPIE 9932, Carbon Nanotubes, Graphene, and Emerging 2D Materials for Electronic and Photonic Devices IX 2016; article number: 99320A.
[3] Bártolo PJ, Almeida H, Rezende R, Laoui T and Bidanda B. Advanced processes to fabricate scaffolds for tissue engineering. Virtual Prototyping & Bio Manufacturing in Medical Applications, B. Bidanda and P. J. Bártolo, Eds., Springer, New York, NY, USA, 2008.
[4] Gibson L. Rapid prototyping: from product development to medicine and beyond. Virtual and Physical Prototyping 2006; 1 (1): 31–42.
[5] Hutmacher DW, Schantz T, Zein I, Ng KW, Teoh SH and Tan KC. Mechanical properties and cell cultural response of polycaprolactone scaffolds designed and fabricated via fused deposition modeling. Journal of Biomedical Materials Research 2001; 55 (2): 203–216.
[6] Mateus AJ, Almeida HA, Ferreira NM et al. Bioextrusion for tissue engineering applications. Virtual and rapid manufacturing, P. J. Bartolo, Ed., London, UK, Taylor & Francis, 2008.
[7] Ceretti E, Ginestra PS, Ghazinejad M, Fiorentino A, Madoub M. Electrospinning and characterization of polymer-graphene powder scaffolds, CIRP Annals 2017; 66(1). In press.
[8] Zein I, Hutmacher DW, Tan KC, Teoh SH. Fused Depositiong Modeling of Novel Scaffold Architectures for Tissue Engineering Applications, Biomaterials 2002; 23 (4): 1169-1185.
[9] Liu C, Xia Z, Czernuszka JT. Design and development of three-dimensional scaffolds for tissue engineering, Chemical Engineering Research and Design 2007; 85 (7): 1051-1064.
[10] Shor L, Guceri S, Wen X, Gandhi M. and Sun W. Fabrication of three-dimensional polycaprolactone/hydroxyapatite tissue scaffolds and osteoblast-scaffold interactions in vitro. Biomaterials 2007; 28 (35): 5291–5297.
[11] Vozzi G, Rechichi A, Dini F et al. PAM-microfabricated polyurethane scaffolds: in vivo and in vitro preliminary studies. Macromolecular Bioscience 2008; 8 (1): 60–68.
[12] Lim TC, Bang CP, Chian KS and Leong KF. Development of cryogenic prototyping for tissue engineering. Virtual and Physical Prototyping 2008; 3 (1): 25–31.
[13] Sobral JM, Caridade SG, Sousa RA, Mano JF, Reis RR. Three-dimensional plotted scaffolds with controlled pore size gradients: Effect of scaffold geometry on mechanical performance and cell seeding efficiency. Acta Biomaterialia 2010; 7 (3): 1009-1018.
[14] Domingos M, Dinucci D, Cometa S, Alderighi M, Bartolo PJ., Chiellini F. Polycaprolactone Scaffolds Fabricated via Bioextrusion for Tissue Engineering Applications. International Journal of Biomaterials 2009; Article ID 239643, 9 pages.

[15] Steffens D, Rezende RA, Santi B, de Sena Pereira FDA, Neto PI, da Silva JVL, Pranke P. 3D- printed PCL scaffolds for the cultivation of mesenchymal stem cells. Journal of Applied Biomechanics and Functional Materials 2016; 14-1: 19-25.
[16] Davila JL, Freitas MS, Neto PI, Silveira ZC, de Silva JVL, d'Avila MA. Software to generate 3-D continuous printing paths for the fabrication of tissue engineering scaffolds. International Journal of Advanced Manufacturing Technology 2016; 84-5-8: 1671-1677.
[17] Loh QL, Choong C. Three-dimensional scaffolds for tissue engineering applications: role of porosity and pore size. Tissue Eng. Part B Rev. 2013; 19 -6: 485-502.
[18] http://reprap.org/wiki/PSU_Fab@Home (visited Feb 2017).
[19] Rasband, W.S., ImageJ, U. S. National Institutes of Health, Bethesda, Maryland, USA, http://imagej.nih.gov/ij/, 1997-2014.